Statistical Shape Analysis for Computer Aided Spine Deformity Detection

Gerhard H. Bendels   Reinhard Klein   Mandana Samimi   Alfred Schmitz

University of Bonn
Institute of Computer Science II
Computer Graphics
Römerstraße 164
D-53117 Bonn, Germany

University of Bonn
Department of Orthopaedics
Sigmund-Freud Straße 25
D-53105 Bonn, Germany

ABSTRACT

In this paper we describe a medical application where we exploit surface properties (measured in form of 3D-Range scans of the human back) to derive a-priori unknown additional properties of the proband, that otherwise can only be acquired using multiple x-ray recordings or volumetric scans as CT or MRI. On the basis of 274 data sets, we perform classification using statistical shape analysis methods. Consistent parameterization and alignment is achieved on the basis of only few anatomic landmarks. As our choice of landmarks is easy to detect on the human body, our approach is feasible for screening applications that can be expected to have much impact on the early detection and later treatment of spine deformities, in particular scoliosis.

Keywords   Statistical Shape Analysis, PCA, Medical Assistance, Scoliosis

1 Introduction and Previous Work

Anthropometric investigations offer interesting approaches to determine etiologic factors of trunk deformities in children. Idiopathic scoliosis is the common spine deformity in prepuberal children [AD85]. Some anthropometric parameters are known as risk factors for developing scoliosis or for scoliosis progressing [HKHDL94, LLFP98, NHSP93, NSL+85]. Early detection of these risk factors could help to prevent developing or progressing of scoliosis by early onset of therapy. Therefore there is a need for screening investigations. In previous studies, anthropometric data was collected mostly by manual measurements [LLFP98, NHSP93]. That means that anthropometric studies are time-consuming and require high personnel expenditures. In screening programs we need an efficient perception and evaluation of anthropometri-

cal data without high personnel costs. Due to its non-invasiveness, accuracy and acquisition speed, recording range-images with laser range scanners seems appropriate for such screening applications [SGWS02].

Figure 1: Conventional radiograph (A) and Magnetic resonance (MR) total spine imaging (B,C), exhibiting the flattening effect of probands being in a supine position during recording.[SJK+01]

The non-invasiveness is of particular importance, since X-ray studies to verify clinical findings in patients with scoliosis and other deformities of the spine are associated with considerable radiation exposure as well as a variety of other problems, particularly as regards assessing disease progression. As close monitoring of the scoliosis is required when the greatest growth of the spine occurs, around puberty and early adolescence, there are obvious concerns that repeated radiographs result in an excessive radiation burden, especially to the developing breast tissue in girls. Nash et al. [NGBP79] estimated that 22 radiographic examinations are performed in the course of scoliosis management.

Therefore, there is a necessity for techniques to reduce the frequency in which x-ray recordings have to be made – if not render them unnecessary. In medical applications, there has consequently been an increasing effort replacing the x-ray examination by other techniques. Inter alia, researchers have investigated MRI-techniques [SJK+01] to assess, visualize, and monitor scoliotic spine deformities. Nevertheless these techniques are not always suitable: Due to the expensiveness and time-intensity of the data acquisition procedure this method is not feasible in screening applications. Moreover, during the CT- or MRT-data acquisition process the proband is in a supine position (see figure 1). This way, e.g. leg length discrepancy, a potent cause for postural scoliosis, is not easily detected, whereas apparent if the proband is in an upright position.

Hence, in the course of the past few years a number of alternative, supplementary spinal diagnostic procedures have been developed which are based on analysis of the surface of the back: Photogrammetry/raster stereometry [LHH+98, DH94], opTRImetric system, ISIS system, video raster stereometry (formetrics), ultrasound-guided spine analysis (Zebris) and ultrasound topometry [AMVK00, RS85]. In particular, [DH94] has used structured light to reconstruct the surface of the proband's back, and produced promising results in assessing the degree of scoliosis, although – lacking anatomical landmarks by which the data sets can be robustly aligned – with yet large error margins.

Not only in medical applications, also in the area of computer graphics, creating computable models of the human body or parts thereof has fascinated researchers over the past decades. As the human eye is especially sensitive in detecting unrealistically modelled human bodies, modelling particularly faces from scratch is an almost infeasible task. Therefore, anthropometric data acquired on or from real human beings has been used for modelling. In [DMS98] statistical distribution of a collection of predetermined facial measurements is used to determine the likelihood of a mod-

elled face, thereby effectively restricting the range of allowable models to constraints derived from a set of input faces. Also focussing on faces, Blanz and Vetter introduced the much celebrated morphable face model [BV99]. Key contribution of their approach is deriving a full correspondence between dense polygonal mesh approximations to the faces using texture information and optical flow techniques. With the face meshes in full correspondence, they perform a principal component analysis identifying correlation and the amount of variation contained in the set of input prototype faces. Although faces seem to be of particular interest to the research community, also the whole body has been subject to research [SMT03, ACP03]. Allen et al. [ACP03] present a human body model that was generated using full body scans acquired in the CAESAR project. The main challenge here was to derive the full correspondence between the body scans. To this end, markers were attached to the probands before scanning. Consistent parametrization was then achieved by fitting a predetermined template mesh to the body scan, where the objective function to be minimized during fitting evaluated the misalignment of the given marker point positions as well as the misalignment of automatically detected geometric features.

Our approach is similar to [BV99] and [ACP03] in the sense, that we aim at deriving a model of the human back such that important information concerning the spine deformity can be won from the 3D-surface information only. Nevertheless, focussing on this application field, our approach is conceptually simpler and very easy to implement. Moreover, our approach relies only on the use of few anatomic landmarks to derive both a robust correspondence between surface points and a robust alignment method. A further important aspect is that we, in contrast to previous approaches, exploit machine learning techniques for classification.

The rest of the paper is organized as follows: We will describe the data acquisition process in section 2. The alignment process required to normalize the data before it can be statistically analysed (section 4) is described in detail in section 3. After the presentation of the results achieved with our approach (section 5), the paper is concluded with final remarks and some hints at future directions of research in section 6.

2 Data Acquisition

Our data basis consists of 3D-scans taken from 109 patients, part of which undergoing scoliosis treatment, others only monitoring. Additionally, in a medical screening cooperation with a local school, we have scanned 165 pupils with no known spine deformity (as they have not been undergoing orthopedic examination beforehand).
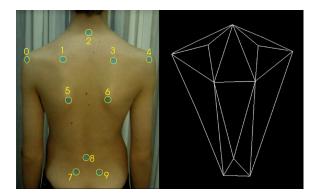
Figure 2: Anatomic landmarks are labelled by an orthopedist. Geometric positions of the landmarks allow consistent coarse mesh generation.

Before scanning, every proband was examined by an orthopedist specialized on spine deformity, who also labelled anatomic landmarks with adhesive markers. These anatomic landmarks (see also figure 2) were chosen for anatomical expressivity and robust detection:

- The spinous process of C7 (2)

- The acromial angle (0,4)

- The superior angle of the scapula (1,3)

- The inferior angle of the scapula (5,6)

- The spinous process of L4 (8)

- The posterior superior iliac spine (7,9)

Note that despite recent advances in 3D-Feature detection the placement of a few marker points to label anatomic landmarks cannot be replaced by automatic feature detection mechanisms as some anatomic landmarks (especially the posterior superior iliac spine and the spinous process of L4) are often covered by soft tissue and are hence not visible in the surface data. This is of particular hindrance in the case of corpulent probands. On the other hand, labelling can be performed not only by specialized physicians but also by trained personnel, such as teachers in schools – a fact that is vital if our system is to be applied in screening applications. During the data acquisition we let physicians do the labelling in order to be able to use their classification statement in the statistical learning stage.

The anatomic landmarks themselves form the vertices for a coarse mesh approximation of the back surface recorded in the range scans. In order to capture the geometric variability contained in the back surface, we construct additional landmarks for our mesh. Following the nomenclature from [DM98], we call

these *Pseudo Landmarks*. In order to produce consistently parameterized meshes for the whole set of range images needed for the statistic analysis, we perform semi-uniform subdivision on the coarse mesh (see figure 3), updating the geometry information with information from the range images. Please note that other
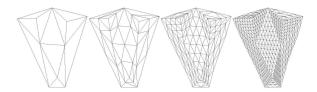

Figure 3: The coarse mesh is semi-uniformly subdivided to produce additional Pseudo Landmarks for the statistical analysis, thereby constructing a consistently parameterized surface approximation.

approaches for mesh re-parametrization as suggested e.g. in [PSS01],[KS04] or [SAPH04] are also feasible at this stage of our algorithm. But, benefitting from the basically planar geometry of the human back, we found this very simple approach of semi-uniform subdivision to be sufficient for our the ensuing application, the statistical analysis. For more complex geometries, e.g. if consistent meshes have to be derived for the entire torso, other strategies will have to be applied. Of course, it is also possible to fit an appropriate template mesh to the range images, as was suggested in [ACP03].

Notation

Suppose we have m data sets (*shapes*). In each data set, we have k corresponding feature points (*landmarks*) in 3-space. Each shape can therefore be represented as an $(k \times 3)$-*shape configuration matrix* $\mathbf{X}_i$, $i = 1, ..., m$, where the j-th row $\mathbf{x}_j^i$, $j = 1, ..., k$ denotes the position of the j-th landmark. The respective components of the landmark vector $\mathbf{x}_j^i$ are denoted by x_j^i, y_j^i, and z_j^i. We suppress the shape index i in case the meaning is clear from the context.

3   Shape Alignment

In order to be able to perform statistical analysis on the shape represented by the landmark coordinates, we need to somehow separate shape variability, that we want to detect, from other sources of variation in the data, e.g. scaling or position in space, that are meaningless for our application. Therefore the input data sets have to be aligned and normalized to make them invariant with respect to the corresponding set of transformations. Although in general this transformation set can be chosen arbitrarily [RDRD04], we choose as invariance set the set of Euclidean similarity transformations, since, according to the shape definition of
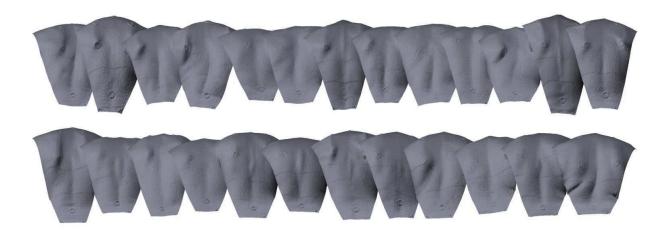
Figure 4: Illustration of the shape space after the reconstruction stage: 25 random examples of the overall 274 reconstructed consistent meshes
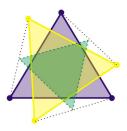

Figure 5: Two identical shapes only differing w.r.t. their rotation (blue and yellow, solid). Without alignment, the mean shape (green, dashed) defined by the arithmetic mean of the respective landmarks would be considerably smaller in size – and even degenerate to a point, had the rotation been about 180 degrees.

Kendall [Ken77], *a shape is all the geometrical information that remains when location, scale, and rotational effects are filtered out*. This means that for each shape $\mathbf{X}$, we have to find an appropriate *scale* $s(\mathbf{X})$, *translation* $\mathbf{d}(\mathbf{X})$, and *rotation* $\mathbf{R}(\mathbf{X})$.
In our algorithm, we will use an alignment approach that combines ideas of two classic alignment approaches, both of which we will shortly describe in the following. For a more thorough covering of alignment approaches, the reader is referred to the extensive literature in this field, e.g. [DM98, Boo86, Sch66], and [Goo91]. A nice introduction is also given in [SG02].

According to Bookstein [Boo84, Boo86] invariance with respect to the Euclidean similarity transformations can be achieved for planar shapes by translating, rotating and scaling each shape such that a pair of landmarks (the so-called baseline) is mapped to predetermined positions. The major drawback of this approach is that it is very sensitive to errors in the baseline landmarks and also, if these are determined automatically, e.g. as points of maximal curvature or as

having the maximum distance, to misidentification.

Therefore, a more robust alignment approach has become popular under the name Procrustean Analysis [Sch66]. The basic idea in Procrustean analysis is to find the required similarity transformations through objective function minimization. This objective function can be defined choosing an appropriate shape distance measure and an appropriate reference shape, with respect to which the distance measure is evaluated. One popular choice for the reference shape is the mean shape

$$\overline{\mathbf{X}} = \frac{1}{m} \sum_{i=1}^{m} \mathbf{X}_i,$$

where on the right hand side, the $\mathbf{X}_i$ have to be aligned in order to be able to compute the "true" mean shape. To solve this hen-and-egg problem, defining the reference shape and aligning the shape configurations is usually understood as an iterative process of aligning all data sets to an *estimated* mean shape $\mathbf{Z}$, updating the mean $\overline{\mathbf{X}}$ and iterating:

---

findMean($\mathbf{X}_1, \ldots, \mathbf{X}_m$, $\mathbf{Z}$)
while $\mathbf{Z}$ changes **do**
    for all $i = 1, \ldots, m$ **do**
        align $\mathbf{X}_i$ with $\mathbf{Z}$;
    end for
    update $\mathbf{Z}$;
end while

An obvious choice for the shape distance measure, required to qualify the optimality of a transformation, is the sum of the squared distances between the corre-
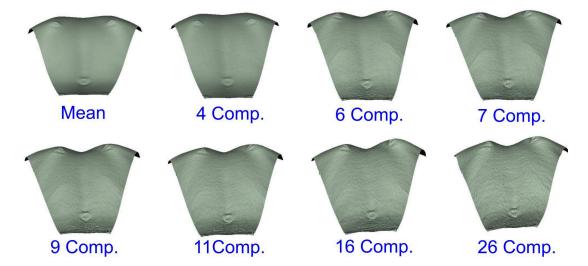
Figure 6: The mean value $\overline{\mathbf{X}}$ and the reconstruction of an example configuration using the denoted numbers of components.

sponding landmarks:

$$D(\mathbf{X}, \mathbf{Y})^2 = \sum_{j=1}^{k} (\mathbf{x}_j - \mathbf{y}_j)^2$$

As this is the same distance measure that is used in the registration of two point sets using the original iterative closest pairs (ICP)-Algorithm, this distance measure leads to a method that is just as susceptive to run into local minima for all but good initial positions. Hence, using this distance measure, shapes have to be roughly pre-aligned, to avoid misalignments. In addition to that, this approach is especially suitable if applied to data sets with uniform landmark confidence, whereas in our case, especially landmarks 2 and 8 (see 2) are of higher confidence compared to the remaining landmarks.

Hence we propose a hybrid approach to compute the similarity transformations given by $(s, \mathbf{d}, \mathbf{R})$:

Translation invariance is achieved by moving the centre of gravity to the origin, i.e. for a configuration $\mathbf{X}$ we compute the centroid

$$\mathbf{d}(\mathbf{X}) = \frac{1}{k} \sum_{j=1}^{k} \mathbf{x}_j.$$

This transformation can conveniently be performed by pre-multiplying $\mathbf{X}$ by the $k \times k$-centring matrix $\mathbf{C} = \mathbf{I}_k - \frac{1}{k} \mathbf{1}_k \mathbf{1}_k^T$, where $\mathbf{I}_k$ is the $k \times k$ identity matrix and $\mathbf{1}_k$ is the k-vector of ones.

Gaining **rotation invariance** is a two-stage procedure in our approach: First, each shape is rotated such that the best-fitting plane of the landmarks in three-space (in a least-squares sense) is rotated to the plane defined by $z = 0$. Since the first stage does not yet determine a unique rotation, a second rotation (around the z-axis) is determined for the second stage. Accounting for the varying confidence in the landmarks, we define a generalized bookstein baseline as the best fitting line to the set of points given by

$$\left\{ p_2, \; p_8, \; \frac{1}{2}(p_7 + p_9), \; \frac{1}{6}(p_0 + p_1 + p_3 + p_4 + p_5 + p_6) \right\}$$

(see figure 2). This special baseline selection was motivated by the fact that the landmarks 2 and 8 (spinous process of C7 and L4), and to a lesser extent landmarks 7 and 9 (posterior superior iliac spine) can be detected very confidently and more robustly than the others.

In the second stage, we therefore rotate each shape such that the projection of this baseline to the plane $z = 0$ is rotated to be parallel to the y-axis.

Please note, that the parameters for the described similarity transformations can very conveniently computed by applying a principal component analysis to the set of anatomic landmarks (for the first stage) or to the set of points described above (for the second stage).

Scale invariance is simply obtained by setting the Euclidean distance between landmarks 2 and 8 to be of unit length.

4 Statistical Analysis

After the shape alignment, the set of shape configurations, consisting of the coordinates of the anatomic and the pseudo landmarks, is fit to be analysed by standard statistical analysis methods. In the following, the shapes will be represented as $(3k)$-dimensional column vectors, which are for simplicity also denoted by $\mathbf{X}_i$, $i = 1, \ldots, m$, as they contain exactly the same information as the $(k \times 3)$-configuration matrices.

In order to reduce dimensionality of the data set for ensuing classification steps we perform a principal component analysis (PCA) on the set of configurations.

As a result from the PCA, we get a set of vectors $\mathbf{e}_1, \ldots, \mathbf{e}_{3k}$ with $||\mathbf{e}_i|| = 1$, $\forall i = 1, \ldots, 3k$, and scalars $\lambda_1, \ldots, \lambda_{3k}$ with $\lambda_i \geq \lambda_{i-1}$, $\forall i = 2, \ldots, 3k$ as the eigenvectors and eigenvalues of the corresponding covariance matrix

$$\mathbf{S} = \frac{1}{m} \sum_{i=1}^{m} (\mathbf{X}_i - \overline{\mathbf{X}})(\mathbf{X}_i - \overline{\mathbf{X}})^T,$$

where $\overline{\mathbf{X}}$ is the mean shape (see section 3). The principal components $\mathbf{e}_i$ form a basis of the shape space spanned by the input configurations, and hence we have for any shape configuration $\mathbf{X}$ and a suitable weight vector $\mathbf{w} = \mathbf{w}(\mathbf{X}) \in \mathbb{R}^m$

$$\mathbf{X} = \overline{\mathbf{X}} + \sum_{i=1}^{m} w_i \mathbf{e}_i,$$

leading to $\mathbf{w}(\mathbf{X})$ being an alternative representation of $\mathbf{X}$ in the PCA-space.
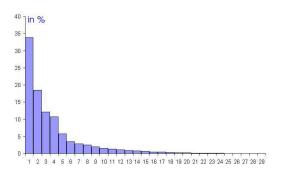

Figure 7: The first 30 main components contribute to over 99 % of the variation in the input data

As can be seen from figure 7 the first 30 components represent already 99 percent of the variation contained in the respective sets (see also figure 6). Therefore, we truncate the weight vectors $\mathbf{w}$ after the 30th component, neglecting the contribution of the principal components $\mathbf{e}_{31}$ to $\mathbf{e}_{3k}$.

Support Vector Machine Approach

Having dramatically reduced the dimension of the data vectors, we are now ready to apply Support Vector Machine classification to our data.

The concept of support vector machines, introduced in [BGV92] and [Vap98] is to find separating planes in high-dimensional vector spaces of labelled sample data. In our setting, the data vectors $(\mathbf{w}, \ell)$ consist of the PCA weight vectors $\mathbf{w}_i$, $i = 1, \ldots, m$

of the back (called *instances*) and appropriate labels $\ell \in -1, 1$ declaring if the corresponding proband was "affected by spine deformity" or "no abnormality detected" (NAD). The basic idea is then, that the *classification function*

$$f : \mathbb{R}^{3k} \mapsto \{-1, 1\}$$

is known for a certain set of instances, called the *learning set*, and unknown otherwise. In our setting, we use linear discriminants a.k.a. *perceptron* as classification function:

$$f(\mathbf{w}) = \langle \mathbf{u}, \mathbf{w} \rangle + b,$$

where $\mathbf{u}$ and b are the parameters that have to be learned from the training examples in the learning set. In addition to that, we have also investigated the effect of decision functions non-linear in $\mathbf{w}$, i.e.

$$f(\mathbf{w}) = \sum_{\nu=1}^{N} \alpha_\nu K(\mathbf{w}_\nu, \mathbf{w}) + b,$$

where N is the number of instances in the learning set and K the radial basis function

$$K(\mathbf{w}_\nu, \mathbf{w}) = \exp(-\gamma ||\mathbf{w}_\nu - \mathbf{w}||^2)$$

with $\gamma > 0$. The decision rule is defined to be $sgn(f)$. As stated before, we investigated the statistical coherence of an overall set of single shot scans of 274 probands, 109 of which were attending scoliosis consultations, the remaining 165 with no a-priori known spine deformity. All probands have been examined and the data sets have correspondingly been labelled "affected" or "NAD". On the basis of this data, we have performed a cross-validation test [CST03], with a preceding grid search for appropriate parameters, as suggested in [HCL04]. For a detailed description of the maximum margin training algorithm, see [BGV92].

5   Results and Conclusions

In this paper, we have described a medical application in which we exploited range images of the human back to derive a computer aided spine deformity detection system. To this end, we recorded an extensive set of range scans of probands with a small set of marked feature points. These feature point markers represent landmarks that cannot be detected by automatic 3d feature detection, as they are often covered by soft tissue, esp. for corpulent probands, but are easy to be found on the real human body. Using these landmarks for consistent parameterization of the polygonal mesh approximations and for aligning the shapes prior to the statistical analysis, we achieved the good results given in table 1, which is in the order of precision a specialized physician would achieve in a screening application and constitutes an improvement over the current

# Folds	⊘Precision	
	linear	rbf
2	92,4812	92,8571
5	92,1053	92,4812
10	92,1053	92,4812
20	92,1053	92,8571
50	92,1053	92,8571

Table 1: Results of the cross validation test using linear or radial basis function-based decision functions. "#Folds" denotes the number of subsets the set of all instances is divided into. (#Folds-1) of these subsets are used for learning, the remaining 1 for testing. "⊘Precision" gives the average percentage of correctly classified instances.

state-of-the-art. This stresses the feasibility of our approach for screening applications, as the markers can easily be applied by trained personnel (e.g. teachers in school) whereas traditional medical classification has to be performed by specialized physicians.

To separate shape variability from variation in pose or scale, the consistently parameterized data sets are normalized in our approach using a novel alignment procedure that is, while benefitting from ideas both of the so-called Procrustean analysis and the alignment using Bookstein-coordinates, simple in concept and easy to implement.

Although so far we applied statistical analysis in an *inter-proband* manner, i.e. giving insight over ones shape characteristics in comparison to the shape space of human backs, our method can naturally be extended to an *intra-proband* examination: By validating recurrent range scanning of one proband, our morphable back model can be used to assess the impact and effect of scoliosis treatment using braces or surgery, and hence serve as a monitoring tool.

6 Future Work

The results achieved from the classification algorithm are encouraging such that we expect the methods presented in this paper to deliver not only qualitative but also quantitative results. The results also prove that surface topography would reflect Cobb angle[1] status with sufficient reliability, but the error margins achieved in previous approaches [GKM+01] are yet wide. We believe that with our approach, reliability and precision of surface-deduced Cobb angle estimation can be significantly increased.

---

[1]The Cobb Angle is the classical measure to describe scoliosis quantitatively as depicted in fig. 1.

References

[ACP03]   Brett Allen, Brian Curless, and Zoran Popovic. The space of human body shapes: reconstruction and parameterization from range scans. *ACM Trans. Graph.*, 22(3):587–594, 2003.

[AD85]   I.A. Archer and R.A. Dickson. Stature and idiopathic scoliosis. a prospective study. *Journal of Bone Joint Surg*, 67:185–188, 1985.

[AMVK00]   V. Asamoah, H. Mellerowicz, J. Venus, and C. Klockner. Measuring the surface of the back. value in diagnosis of spinal diseases. *Orthopade*, 29:480–489, 2000.

[BGV92]   Bernhard E. Boser, Isabelle M. Guyon, and Vladimir N. Vapnik. A training algorithm for optimal margin classifiers. In *Proceedings of the fifth annual workshop on Computational learning theory*, pages 144–152. ACM Press, 1992.

[Boo84]   F.L. Bookstein. A statistical mehod for biological shape comparisons. *Journal of Theoretical Biology*, 107:475–520, 1984.

[Boo86]   F.L. Bookstein. Size and shape spaces for landmark data in two dimensions (with discussion). *Statistical Science*, 1:181–242, 1986.

[BV99]   Volker Blanz and Thomas Vetter. A morphable model for the synthesis of 3d faces. In *Proceedings of the 26th annual conference on Computer graphics and interactive techniques*, pages 187–194. ACM Press/Addison-Wesley Publishing Co., 1999.

[CST03]   Nello Cristianini and John Shawe-Taylor. Support vector and kernel methods. *Intelligent data analysis*, pages 169–197, 2003.

[DH94]   B. Drerup and E. Hierholzer. Back shape measurement using video rastersterography and three-dimensional reconstruction of spinal shape. *Clinical Biomechanics*, 9(1):28–36, 1994.

[DM98]   I. L. Dryden and Kanti V. Mardia. *Statistical Shape Analysis*. John Wiley and Sons, 1998.

[DMS98]   Douglas DeCarlo, Dimitris Metaxas, and Matthew Stone. An anthropometric face model using variational techniques. In *Proceedings of the 25th annual conference on Computer graphics and interactive techniques*, pages 67–74. ACM Press, 1998.

[GKM+01] C.J. Goldberg, M. Kaliszer, D.P. Moore, E.E. Fogarty, and F.E. Dowling. Surface topography, cobb angles, and cosmetic change in scoliosis. *Spine*, 26:E55–63., 2001.

[Goo91] C. Goodall. Procrustes methods in the statistical analysis of shape. *Journal Royal Statistical Society Series B-Methodological*, 53(2):285–339, 1991.

[HCL04] Chih-Wei Hsu, Chih-Chung Chang, and Chih-Jen Lin. A practical guide to support vector classification. http://www.csie.ntu.edu.tw/ cjlin/libsvm/index.html, 2004.

[HKHDL94] A.A. Hazebroek-Kampschreur, A. Hofman, A.P. Dijk, and B. Ling. Determinants of trunk abnormalities in adolescence. *Int J Epidemiol*, 23:1242–1247, 1994.

[Ken77] D.G. Kendall. The diffusion of shape. advances in applied probability., 1977.

[KS04] Vladislav Kraevoy and Alla Sheffer. Cross-parameterization and compatible remeshing of 3d models. *ACM Trans. Graph.*, 23(3):861–869, 2004.

[LHH+98] U. Liljenqvist, H. Halm, E. Hierholzer, B. Drerup B, and M. Weiland. 3-dimensional surface measurement of spinal deformities with video rasterstereography. *Z. Orthop Ihre Grenzgeb*, 136:57–64, 1998.

[LLFP98] R. LeBlanc, H. Labelle, F. Forest, and B. Poitras. Morphologic discrimination among healthy subjects and patients with progressive and nonprogressive adolescent idiopathic scoliosis. *Spine*, 23:1109–1115, 1998.

[NGBP79] C.L. Nash, E.C. Gregg, R.H. Brown, and K. Pillai. Risks of exposure to x-rays in patients undergoing long-term treatment for scoliosis. *The Journal of Bone and Joint Surgery*, 61(3):371–374, 1979.

[NHSP93] M. Nissinen, M. Heliovaara, J. Seitsamo, and M. Poussa. Trunk asymmetry, posture, growth, and risk of scoliosis. a three-year follow-up of finnish prepubertal school children. *Spine*, 18:8–13, 1993.

[NSL+85] H. Normelli, J. Sevastik, G. Ljung, S. Aaro, and A.M. Jonsson-Soderstrom. Anthropometric data relating to normal and scoliotic scandinavian girls. *Spine*, 10:123–126, 1985.

[PSS01] Emil Praun, Wim Sweldens, and Peter Schroeder. Consistent mesh parameterizations. In *Proceedings of the 28th annual conference on Computer graphics and interactive techniques*, pages 179–184. ACM Press, 2001.

[RDRD04] B. Romaniuk, M. Desvignes, M. Revenu, and M.-J. Deshayes. Shape variability and spatial relationships modeling in statistical pattern recognition. *Pattern Recognition Letters*, 25(2):239–247, 2004.

[RS85] A. Rohlmann and J. Siraky. Reproducibility of surface measurements of the back using the optrimetric method. *Z Orthop Ihre Grenzgeb*, 123:205–212, 1985.

[SAPH04] John Schreiner, Arul Asirvatham, Emil Praun, and Hugues Hoppe. Inter-surface mapping. *ACM Trans. Graph.*, 23(3):870–877, 2004.

[Sch66] Peter H. Schoenemann. A generalized solution of the orthogonal procrustes problem. *Psychometrika*, 31:1–10, 1966.

[SG02] M. B. Stegmann and D. D. Gomez. A brief introduction to statistical shape analysis, March 2002. Images, annotations and data reports are placed in the enclosed zip-file.

[SGWS02] Alfred Schmitz, H. Gabel, H.R. Weiss, and Ottmar Schmitt. Anthropometric 3d-body scanning in idiopathic scoliosis. *Z Orthop Ihre Grenzgeb*, 140:632–636, 2002.

[SJK+01] Alfred Schmitz, Ursula E. Jaeger, Roy Koenig, Joerg Kandyba, Ulrich A. Wagner, Juergen Giesecke, and Ottmar Schmitt. A new mri technique for imaging scoliosis in the sagittal plane. *European Spine Journal*, 10(2):114–117, April 2001. Issn: 0940-6719 (Paper) 1432-0932 (Online).

[SMT03] Hyewon Seo and Nadia Magnenat-Thalmann. An automatic modeling of human bodies from sizing parameters. In *Proceedings of the 2003 symposium on Interactive 3D graphics*, pages 19–26. ACM Press, 2003.

[Vap98] V.N. Vapnik. Statistical learnig theory. Wiley, New York, 1998.